Fermilab FERMILAB-CONF-04-438-E DECEMBER 2004

Physics with Taus at CDF

Alexei N. Safonov[a], for CDF Collaboration

[a]Department of Physics, University of California at Davis,
One Shields Ave., Davis, CA 95616, USA

In this contribution, we describe the hadronic tau reconstruction and identification procedures adopted by the CDF experiment at Fermilab and present an overview of physics studies using tau leptons that are underway at CDF. Recent results using data obtained from Run II of the Tevatron are presented and include precision electroweak measurements as well as studies aimed at beyond Standard Model searches for new particles and interactions.

1. Introduction

In Run II of the Tevatron, tau leptons have an important role in electroweak measurements and studies of top quark properties. But most remarkably, it has a very special place in searches for new phenomena. For the latter case, both Higgs and Supersymmetry phenomenology predict signatures with multiple taus.

Amid a strong physics motivation for exploring data with taus in the final state, tau reconstruction at hadron colliders remains a notoriously difficult task in terms of distinguishing interesting events from backgrounds dominated by multi-jet production with its enormous cross section. Another related challenge is providing efficient triggering for events with hadronic taus while keeping trigger rates at levels sustainable by the trigger system.

In this contribution, we describe tau reconstruction and identification procedures adopted by the CDF experiment, discuss hadronic tau triggers and present preliminary physics results.

2. Hadronic Tau Reconstruction

Here, we give only a brief description of the detector sub-systems critical for hadronic tau reconstruction. Full details can be found elsewhere [1]. The CDF central calorimeter consists of electromagetic (CEM) and hadronic (CHA) compartements. Energy measurements are made within projective "towers" that span 0.1 units in pseudorapidity and 15^0 in ϕ. The CEM detector has an embedded multi-wire proportional chamber (CES) located near the shower maximum, which serves for more accurate measurement of the electromagnetic shower spatial position. The CES is also used to reconstruct neutral pions used in tau reconstruction. The primary tracking system is the Central Outer Tracker (COT), a drift chamber consisting of four axial and four stereo superlayers of 12 wires each (stereo wires are tilted by 3^0 with respect to the central axis of the detector).

Tau candidates are reconstructed by matching narrow calorimeter clusters with tracks. The calorimeter cluster is required to have E_T of the seed tower above 6 GeV. All adjacent towers with transverse energy above 1 GeV are included in the cluster. The sum of transverse energies of the towers is used as the transverse energy of the tau candidate, $E_T^{\rm cal}$. Only clusters consisting of 6 or less towers are used for tau reconstruction.

2.1. Tracking Reconstruction

Reconstructed tracks that point to the calorimeter cluster are associated with the tau candidate. The highest p_T track associated with the tau is called the *seed track* and defines the axes of the signal and isolation cones. The signal cone is defined as a cone with an opening angle α around the seed track, where

$$\alpha_{\rm trk} = \min(0.17, \max(5\ \ {\rm GeV}/E^{\rm cal}, 0.05)) \qquad (1)$$

This definition takes into account collimation of hadronic tau jets with increasing energy, providing high signal efficiency (see Fig. 1 for illustration) and better background rejection compared to a fixed size cone.

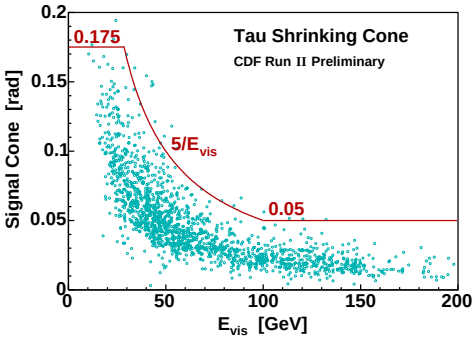

Figure 1. Illustration for the definition of the energy dependent tau signal cone. Points show the angle between the tau seed track and farthest shoulder track for hadronically decaying taus as predicted by the simulation. This definition provides high signal efficiency and stronger background rejection compared to a fixed size cone.

Tau decay modes are often classified by the number of prongs. At CDF, prongs are defined as tracks inside the signal cone of a tau candidate with transverse momentum $p_T > 1$ GeV/c. We require tracks to pass certain quality requirements and, in addition, for a track to be associated with the tau candidate, it is required that the track has z_0 compatible with that of the seed track: $|z_0^{\rm trk} - z_0^{\rm seed}| < 5$ cm.

2.2. π^0 Reconstruction

Next, the π^0 information is added. The raw wire and strip CES clusters are obtained using a clustering algorithm that starts with a seed wire or strip and combines up to 5 wires or strips into a cluster. Then raw strip and wire clusters are matched to each other to form two dimensional CES clusters as illustarted in Fig. 2. In cases when matching is not unique, energy measured in the CES is used to identify which wire and strip clusters are coming from the same cluster. Each matched cluster is called a π^0 candidate if no COT track of $p_T > 1$ GeV/c is found nearby. If only one π^0 candidate is found in a particular calorimter tower, the energy assigned to the π^0 is the full EM energy of this tower minus expected deposited energy from all tracks traversing this tower:

$$E^{\pi^0} = E^{\rm EM} - \sum_{\rm trks} (0.3 + 0.21 \times p), \qquad (2)$$

with all energy units taken to be in GeV. If there are more than one π^0 candidates in the same calorimeter tower, the available EM energy is divided between them proportionally to their respective cluster energies measured by the CES system.

Similar to the track case, for π^0's we define a cone around the seed track

$$\alpha_{\pi^0} = \min(0.17, \max(5\ \ {\rm GeV}/E^{\rm cal}, 0.10))\ , \qquad (3)$$

and all π^0 candidates inside the cone with $E_T >$ 1 GeV are associated with the tau candidate.

2.3. Tau Energy Measurement

The energy of the tau candidate can be measured either using calorimeter information or using reconstructed tracks and π^0's. Due to the relatively low resolution of the hadronic calorimeter, the latter is preferred. The momentum of a tau is defined as the sum of massless four-vectors of all tracks and π^0's associated with the tau candidate:

$$p^\tau = \sum_{\Delta\Theta<\alpha_{\rm trk}} p^{\rm trk} + \sum_{\Delta\Theta<\alpha_{\pi^0}} p^{\pi^0}\ . \qquad (4)$$

The transverse momentum of a tau candidate is defined as

$$p_T^\tau = \sqrt{{p_x^\tau}^2 + {p_y^\tau}^2}\ , \qquad (5)$$

where p_x^τ and p_y^τ are the x- and y-component of the tau momentum four-vector.

In some (relatively rare) cases, a π^0 cannot be reconstructed (e.g. due to dead wires in CES or an accidental overlap of a π^0 with a nearby track). This leads to a mismeasurement of the tau candidate energy. We apply a special correction that detects cases of excessesive EM energy

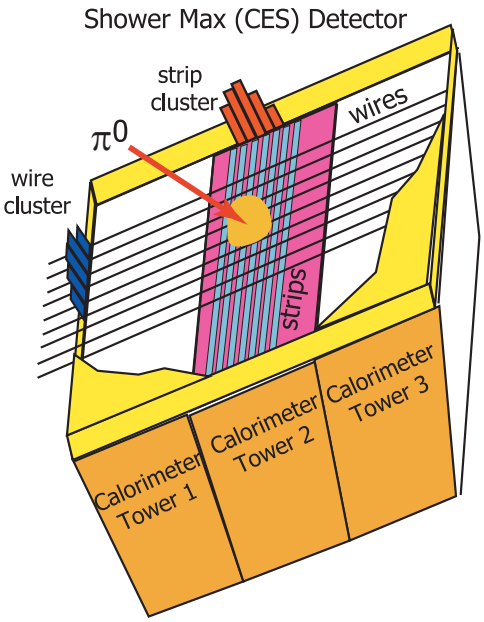

Figure 2. A pictorial illustrating π^0 candidate reconstruction using ShowerMax (CES) detector. Candidates are reconstructed as two dimensional clusters using CES strip and wire information. Spatial position of the candidates is assigned based on CES measurement, and the momentum is determined using EM calorimeter energy deposition.

not assigned to any π^0 candidate and corrects the energy of tau candidates.

2.4. Identification Variables

Several variables useful for discriminating between real taus and background fakes are defined using track and π^0 information.

The visible mass of a tau candidate, $m^{\tau}_{\mathrm{trk}+\pi^0}$, is defined as the invariant mass of the tau momentum four-vector obtained in Eq. 4, before applying the correction for missed π^0's. The track mass of a tau candidate, m^{τ}_{trk}, is defined as the invariant mass of the track-only part of the tau momentum four-vector, Eq. 4. The charge of a tau candidate is defined as a sum of charges of the prongs associated with it:

$$Q^{\tau} = \sum_{\tau \text{ tracks}} Q_{\mathrm{trk}} \ , \tag{6}$$

For discriminating hadronic taus from electrons, a useful variable ξ is defined as

$$\xi = E_T^{had} / \sum_{\tau \text{ tracks}} p_T^{\mathrm{trk}} \ , \tag{7}$$

where E_T^{had} is the transverse energy of the tau candidate calculated using only hadronic deposition in the calorimeter. For electrons, the ξ value is typically small, and this allows substantial suppression of backgrounds with an electron faking a tau.

At hadron colliders, isolation plays a central role in tau identification, as it is the most powerful cut against QCD jet backgrounds. The first kind of isolation is track isolation. We use two varieties of this cut. In the first case we define isolation as a scalar sum of the momenta of all tracks inside a cone of 30^0 around the seed track but outside the signal cone in 3D space:

$$I^{\Delta\Theta}_{\mathrm{trk}} = \sum_{\alpha_{\mathrm{trk}} < \Delta\Theta < 30^0} p_T^{\mathrm{trk}} \ . \tag{8}$$

Note that for a track to be counted in the isolation, it is required that the track has z_0 compatible with that of the seed track: $|z_0^{\mathrm{trk}} - z_0^{\mathrm{seed}}| < 5$ cm. Another kind of isolation, $N^{\Delta\Theta}_{\mathrm{trk}}$, is defined as the number of isolation tracks with $p_T > 1$ GeV/c.

In a similar way, we define the tau candidate π^0 isolation as

$$I^{\Delta\Theta}_{\pi^0} = \sum_{\alpha_{\pi^0} < \Delta\Theta < 30^0} p_T^{\pi^0} \tag{9}$$

Analogously to the track case, we also define N_{π^0} as the number of π^0 candidates in the isolation cone. In all cases, only π^0 candidates that have matches in both wire and strip CES views are used in the isolation.

3. CDF Tau Triggers

The CDF trigger system [1] consists of three levels that are used to reduce the 7.6 MHz

nominal crossing rate to the 50 Hz maximum written to tape. Level 1 is a fully hardware based trigger and has access to tracking information reconstructed in the eXtremely Fast Tracker (XFT), calorimeter energy measurements in each of the trigger towers (trigger tower consists of two calorimeter towers adjacent in η), missing transverse energy and muon stub information. Level 2 is still primarily a hardware trigger, but has software based decision logic. In addition to what is available at Level 1, it has access to calorimeter clusters and tracks reconstructed in the silicon tracker (SVX). Level 3 is a software trigger where a slightly simplified version of the final reconstruction is run, and it has access to most of the information available offline.

CDF currently has five triggers targeting hadronic taus in the final state. We give a brief description of each of them. More information can be found in [4].

The TAU_MET trigger targets events with a hadronic tau candidate and substantial transverse missing energy, e.g. $W \to \tau\nu$. At Level 1, this trigger requires a single tower of $E_T \geq 10$ GeV, at Level 2 it requires a tau candidate defined as a match between a 2D XFT track and a calorimeter cluster with thresholds of $p_T \geq 10$ GeV/c and $E_T \geq 10$ GeV and missing transverse energy of $\not\!\!E_T \geq 20$ GeV. A Level 2 track has to pass track isolaton defined as absence of XFT tracks in $10^0 < \Delta\phi < 30^0$. Level 3 has access to high level objects that are nearly identical to the ones in the offline reconstruction. We require a tau candidate of $E_T \geq 20$ GeV with $m^{\tau}_{\rm trk} < 2$ GeV/c^2 and absence of COT tracks with $p_T > 1$ GeV/c in the 3D annulus of $10^0 - 30^0$ around the tau candidate seed track. In addition, we reapply the requirement of $\not\!\!E_T \geq 20$ GeV.

At Level 1, the DI_TAU trigger requires two towers of $E_T > 5$ GeV. At Level 2 it requires two tau candidates using the same definition as in TAU_MET trigger, but with softer threshold on the seed track, $p_T^{XFT} \geq 6$ GeV/c. At Level 3, each of the two reconstructed tau objects has to pass isolation cut of no tracks in the 3D annulus of $10^0 - 30^0$ around the tau candidate seed track.

In addition to the two abovementioned triggers, CDF has implemented *lepton+track* triggers, which consist of one path, $CEM8\_TRACK5$, targeting *electron + tau* events and two paths, $CMUP8\_TRACK5$ and $CMX8\_TRACK5$, aimed at the *muon + tau* events using two muon subsystems, CMUP and CMX. At Level 1, $CEM8\_TRACK5$ trigger requires at least one trigger tower with EM $E_T > 8$ GeV and a matching XFT track of $p_T > 8$ GeV/c, *muon + track* triggers require a stub in either CMU and CMP or CMX system matched to an XFT track of $p_T > 8$ GeV/c. At Level 2, the triggers confirm presence of an electron or muon candidate and require presence of an additional XFT track of $p_T > 5$ GeV/c. At Level 3, the triggers require a loose lepton (e or μ) candidate and a track isolated by a requirement of no tracks with $p_T > 1.5$ GeV/c in an annulus of $10^0 - 30^0$ around it.

In 2005, we plan to add two *lepton+tau* triggers that will expand the coverage for electrons and muons into the forward direction.

4. Precision Electroweak Measurements

While precision electroweak measurements are important by themselves, they also serve to demonstrate that CDF can successfully reconstruct and identify hadronically decaying taus and correctly predict associated backgrounds.

4.1. $W \to \tau\nu$ Cross Section Measurement

The $W \to \tau\nu$ sample is the largest single source of events enriched with hadronic taus. This analysis uses events collected using the TAU_MET trigger. The offline requirements start by requiring a tau candidate with $p_T \geq 25$ GeV/c and $\not\!\!E_T \geq 25$ GeV. The tau candidate is required to pass the following cuts: $m^{\tau}_{\rm trk+\pi^0} < 1.8$ GeV/c^2, $\xi < 0.15$, followed by isolation requirements $N^{\tau}_{trk} = 0$ and $N^{\tau}_{\pi^0} = 0$. To improve purity of the signal, a *monojet* requirement is imposed requiring no jets of $E_T > 5$ GeV reconstructed in the calorimeter system. This latter cut is found to be very effective in suppressing QCD multi-jet backgrounds that tend to have energy in the forward η regions. Backgrounds are dominated by the QCD jet production when jet fakes a tau and $W \to e$, where electron passes ξ cut either due to

a strong bremstrahlung or late showering in the calorimeter. Jet backgrounds are estimated using a fake rate technique, for other backgrounds MC is found to be sufficiently reliable. We find a good agreement between data and expectations as illustrated in Fig. 3, which shows the track multiplicity of tau candidates in events passing all analysis requirements and demonstrates the characteristic tau shape.

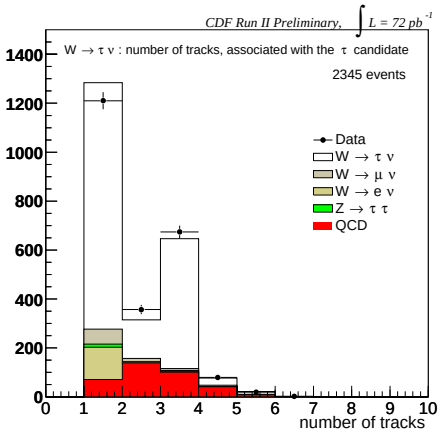

Figure 3. Distribution for the number of tracks assigned to a tau candidate in the selected $W \to \tau\nu$ candidate events.

We measure $\sigma(p\bar{p} \to W)Br(W \to \tau\nu) = 2.62 \pm 0.07(\text{stat}) \pm 0.21(\text{syst}) \pm 0.16(\text{lum})$ *nb*. Comparison of $W \to \tau\nu$ yields to those in $W \to e\nu$ channel allows measurement of the ratio of branchings $Br(W \to \tau\nu)/Br(W \to e\nu) = 0.99 \pm 0.04(stat) \pm 0.07(syst)$. Note partial cancellation of the systematic uncertainties. These results are then used to constrain the ratio of the couplings $g_\tau/g_e = 0.99 \pm 0.02(stat) \pm 0.04(syst)$.

4.2. $Z \to \tau\tau$ Cross Section Measurement

Apart from verifying lepton universality, the measurement of the $Z \to \tau\tau$ cross section has a particular importance as the main irreducible background for most of the Higgs and new phenomena searches. It is a perfect ground for developing techniques for predicting other backgrounds and working out reconstruction and identification techniques. The $Z \to \tau\tau$ cross section measurement can also serve as a normalization and calibration for other analyses.

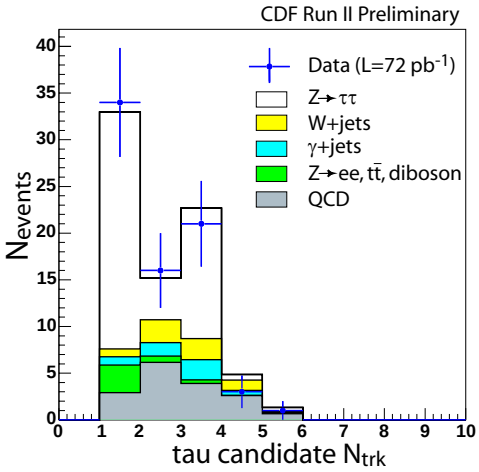

Figure 4. Distribution for the number of tracks assigned to a tau candidate in the selected $Z \to \tau_e\tau_h$ candidate events.

Results presented here refer to the channel with one of the taus decaying into an electron while the other one decays hadronically. Results for muon channel, which is actually easier due to much lower multi-jet backgrounds, are expected to be finalized in the near future. This analysis is based on 72 pb^{-1} of data collected using *electron+track* trigger. Event selection starts with a requirement of at least one good quality isolated electron with $E_T \geq 10$ GeV and at least one hadronic tau candidate with $p_T \geq 15$ GeV/c, both in the central part of the detector. Tau identification cuts are similar to $W \to \tau$ analysis, with the exception of calorimeter isolation that is not used and a looser cut on the tau mass, $m_\tau < 2.5$ GeV/c^2. Tau track isolation cut is $I_{\text{trk}}^{\Delta\Theta} < 1$ GeV/c. To improve purity of the signal, a se-

ries of event topology cuts are applied to remove events with electrons coming from $\gamma-$conversions and $Z \to ee$. Multi-jet and W+jets backgrounds are suppressed using cuts on transverse mass of electron and $\not\!\!E_T$: $M_T(e, \not\!\!E_T) \leq 25$ GeV/c^2, and on vector sum of transverse momenta of electron and $\not\!\!E_T$: $p_T = |\vec{p}_T^{\,e} + \vec{\not\!\!E}_T| > 25$ GeV/c. Figure 4 shows track multiplicity for hadronic taus in selected events indicating an agreement with expectation and also good control of backgrounds.

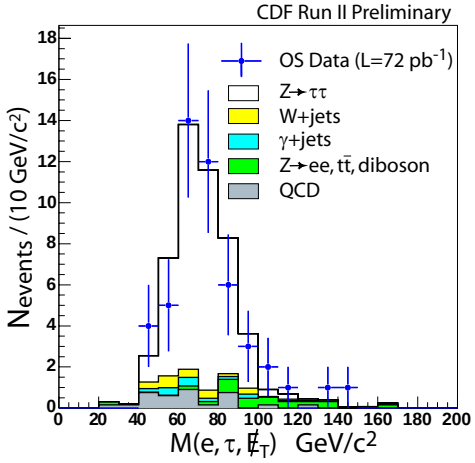

Figure 5. Invariant mass of the $\not\!\!E_T$, electron and hadronic tau system in the selected $Z \to \tau_e \tau_h$ candidate events.

To further improve purity, we apply cuts on the number of tracks in tau candidates to be 1 or 3 and also require $Q_e \cdot Q_\tau = -1$. Final selected events are used to measure the cross-section $\sigma(p\bar{p} \to Z)Br(Z \to \tau\tau) = 242 \pm 48(\text{stat}) \pm 26(\text{syst}) \pm 15(\text{lumi})$. Figure 5 shows the mass spectrum defined as the invariant mass of the sum of electron, tau and $\not\!\!E_T$ four-momenta for the final events.

5. Searches for New Phenomena

In this section, we describe the ongoing studies aimed at searching for new physics beyond the Standard Model.

5.1. MSSM Higgs Decaying to Taus

In the context of the minimal supersymmetric standard model (MSSM) the Higgs sector has two doublets, one coupling to up-type quarks and the other to down-type quarks. There are five physical Higgs boson states, h, A, H and $H^{\pm}$. Masses and couplings are determined by two parameters m_A and $\tan\beta$. In the case of large $\tan\beta$, there is an enhacement for the neutral Higgs production comapred to SM. CDF has performed a search for $H \to \tau\tau$ using approximately 200 pb^{-1} of data and provided a limit in the cross section versus MSSM Higgs mass plane. Compared to searches with b-jets in the final state, di-tau channel has the advantages of much cleaner signature and lower backgrounds.

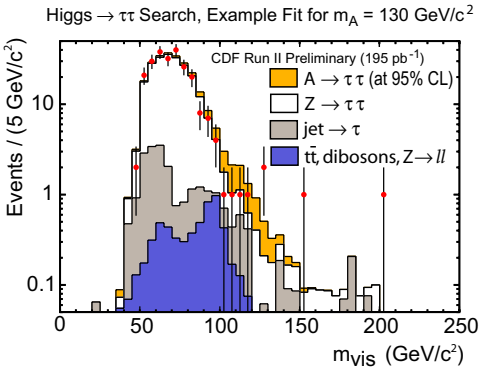

Figure 6. Invariant mass of two taus and $\not\!\!E_T$ distribution in the selected $A \to \tau_{e/\mu}\tau_h$ candidate events. Data is compared to the background predictions and Higgs signal.

This analysis uses 200 pb^{-1} of data collected by *lepton+track* triggers and starts by requiring an electron or muon with $p_T > 10$ GeV/c and a tau candidate of $p_T > 15$ GeV/c. After applying lepton and tau identification cuts, we remove events tagged as $Z \to ee, \mu\mu$, cosmic or $\gamma-$conversions. Two additional cuts are

applied to suppress W+jets and $Z \to \tau\tau$, the largest background for this study: $H_T = p_T(\tau_1) + p_T(\tau_2) + \not\!\!E_T > 50$ GeV and a specially designed cut on the direction and magnitude of $\not\!\!E_T$ with respect to the two tau candidates.

The observed number of events is in agreement with the expectation based on SM predictions (excluding Higgs), Fig. 6 shows the distribution for the invariant mass of the two taus and $\not\!\!E_T$. With no excess, we set a limit on the MSSM Higgs production by fitting the invariant mass distribution using the expected $Z \to \tau\tau$ spectrum and generated templates for Higgs signal at several mass points. Extracted upper limit on the allowed cross-section of $A \to \tau\tau$ is shown in Fig. 7. Currently, we are sensitive to SUSY only at high $\tan\beta$, but we expect a significant improvement with more data becoming available for analisys and better optimization of the event selection.

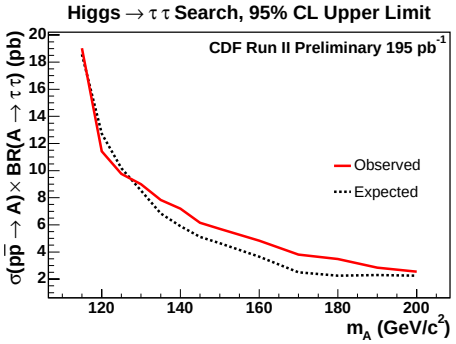

Figure 7. Upper limit (at 95% CL) for the cross-section of $p\bar{p} \to H \to \tau_{e/\mu}\tau_h$ process.

5.2. Search for Z' Decaying to Taus

This analysis is dedicated to a search for high mass tau pairs. Relevant physics scenarios include heavy Z-like resonances (Z') [5], heavy Higgs and R_p-violating SUSY. This analysis is complementary to earlier CDF searches of Z' decaying into electrons and muons.

This analysis uses 200 pb^{-1} of data collected by *lepton+track* and *DI_TAU* triggers and starts by requiring an electron or muon with $p_T > 10$ GeV/c and a tau candidate of $p_T > 25$ GeV/c (or two hadronic taus of $p_T > 25$ GeV/c and $p_T > 10$ GeV/c for the channel with two hadronic taus). After applying lepton and tau identification cuts and removal of events tagged as $Z \to ee, \mu\mu$, cosmic or $\gamma-$conversions, additional cuts are applied to suppress W+jets and $Z \to \tau\tau$ backgrounds: $\not\!\!E_T > 15$ GeV (25 for two hadronic taus mode) and require that the direction of $\not\!\!E_T$ is within 30^0 of the leptonically decaying tau (or lower p_T hadronic tau for the two hadronic tau mode).

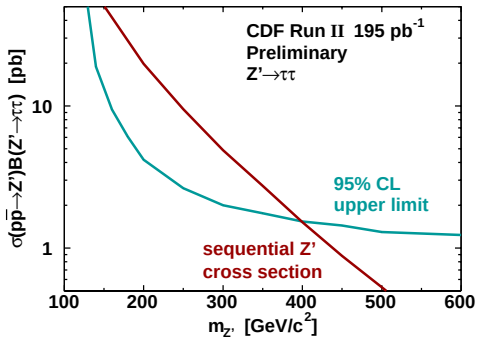

Figure 8. 95% C.L. upper limit on the cross-section of $p\bar{p} \to Z'$ production assuming $Br(Z' \to \tau\tau) = 100\%$ as a function of Z' mass. Comaprison of the exclusion curve to the theoretical prediction allows setting a mass limit above 400 GeV/c^2.

Table 1 shows the comparison of the background predictions with the number of observed events in data. The comparison allows setting an upper limit on allowed cross-section of the $p\bar{p} \to Z'$ process and sets a Z' mass limit as illustrated in Fig. 8.

5.3. Search for Doubly Charged Higgs

Doubly charged Higgs appear in the Left-Right symmetric models [6,7] and in SUSY. CDF has recently published an analysis [8] dedicated to a search for pair produced doubly charged Higgs,

Table 1
Background predictions and the number of observed events in data in the search for high mass Z' decaying into two taus.

Source	$\tau_e\tau_h$	$\tau_\mu\tau_h$	$\tau_h\tau_h$	Total
$Z/\gamma^* \to \tau\tau$	0.56 ± 0.11	0.50 ± 0.10	0.36 ± 0.08	1.42 ± 0.23
$Z/\gamma^* \to ee$	0.16 ± 0.14	0	0	0.16 ± 0.14
$Z/\gamma^* \to \mu\mu$	0	0.50 ± 0.26	0	0.50 ± 0.26
$Jet \to \tau$	0.29 ± 0.14	0.18 ± 0.09	0.28 ± 0.10	0.75 ± 0.19
Total Bkgd	1.01 ± 0.24	1.18 ± 0.30	0.64 ± 0.13	2.83 ± 0.46
Observed	4	0	0	4

$H^{++/--}$, decaying to light leptons (e or μ) showing no evidence for H^{++} yet, and a limit was set for these decay modes. Given that the models allowing for H^{++} do not provide predictions for the branching ratio to lepton species, these limits do not constrain the $H^{++} \to \tau\tau$ channel. Furthermore, indirect limits, e.g. Bhabha scattering, indicate that coupling to e or μ is unlikely to be significant. $H^{++} \to \tau\tau$ remains largely unrestricted for $m_H > 100$ GeV/c^2, e.g. LEP excludes $m_H > 98.5$ GeV/c^2 [9]. At the Tevatron, the main production mechanism for doubly charged Higgs is pair production. An important feature is that the coupling is proportional to β^3 [10], where β is the boost of the Higgs in the center of mass frame. This leads to both Higgs bosons having substantial transverse momenta thus making this process very clean of any backgrounds.

Analysis at CDF starts by requiring two like-sign tau candidates (one decaying leptonically, while another one decays via one of the hadronic modes) and at least one additional tau-style isolated track of opposite charge with respect to the two tau candidates. Of all passing events, events of two distinct categories are preserved for further analysis: (i) like-sign di-tau pair and exactly one good isolated track of opposite sign and (ii) like-sign di-tau pair and two like-sign isolated tracks. Then a set of event topology cuts is applied in order to suppress remaining backgrounds, these cuts include $\not\!\!E_T$, sum of the transverse momenta of the di-tau candidate pairs and the opening angles of the di-tau pairs (the latter is correlated with the mass of the parent Higgs boson). Event topology cuts are optimized for each of the two categories individually to maximize the significance. After opening the box, we will simultaneously fit the observed number of events in each of the two categories for electron and muon channels to set a limit on the cross-section of the H^{++} pair production. The cross-section limit will then be propagated into a mass limit. We expect to make preliminary results of this analysis available in early 2005.

5.4. SUSY Stop Quark Decaying to τ and a b-quark via R-Parity Violating Coupling

Stop quarks, the supersymmetric partners of the top quark, can be pair produced at the Tevatron. In SUSY, if R_p is violated, stops can decay into a b-jet and a τ. This recent CDF analysis has performed a search for stop quarks in this scenario by looking for events with two taus (one hadronic and one leptonic) and two jets. Event selection starts with requiring at least one lepton (electron or muon) with $E_T \geq 10$ GeV and one tau candidate with $p_T^\tau \geq 15$ GeV/c. Identification cuts are similar to those in the $Z \to \tau\tau$ analysis, while lepton isolation requirements are slightly looser ($I_{\rm trk}^{e/\mu} < 2$ GeV/c) to accomodate the presence of two hard jets in stop events. After initial selection, several event-level cuts are used to suppress contamination of $Z \to ee(\mu\mu)$, cosmic and $\gamma-$conversion events followed by a cut on $Y_T = |p_T^l + p_T^\tau + \not\!\!E_T| > 85$ GeV/c. Events passing selection criteria are then categorized according to the number of jets with $E_T \geq 15$ GeV and whether they satisfy a require-

ment of $M_T(l, \not\!\!E_T) < 35$. We use events in regions with $n_{jet} = 0$ (dominated by backgrounds) and $n_{jet} \geq 2$ (most of the signal) to perform a simultaneous fit for possible signal. In the region with $n_{jet} \geq 2$ and $M_T < 35$ GeV/c^2 the background prediction is 2.5 (2.2) events in electron (muon) channel; after opening the box, we have found 2(3) events in data in agreement with the background expectations. Figure 9 shows the distribution for the number of jets for final events that are additionally required to pass $M_T < 35$ GeV/c^2 cut showing good agreement of data and expected backgrounds.

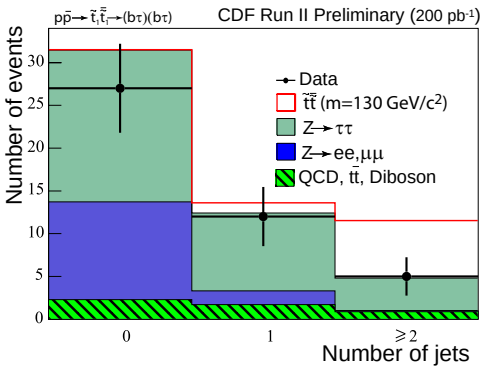

Figure 9. Distribution for the number of jets in stop candidate events with $M_T(l, \not\!\!E_T) < 35$ GeV/c^2 compared with the background expectation and expected spectrum of the stop events with $M(\tilde{t}_1) = 130$ GeV/c^2. We conclude that the data is consistent with the predicted SM backgrounds.

With no excess of events found over the SM expectation, we set a 95% C.L. limit on the production cross-section of this process, as shown in Fig. 10, and also a limit on the mass of the stop quark, $M(\tilde{t}_1) > 129$ GeV/c^2. Note that the results of this search are fully applicable to the case of the scalar leptoquark, because the dynamics and the expected cross section are almost indistinguishible from stop.

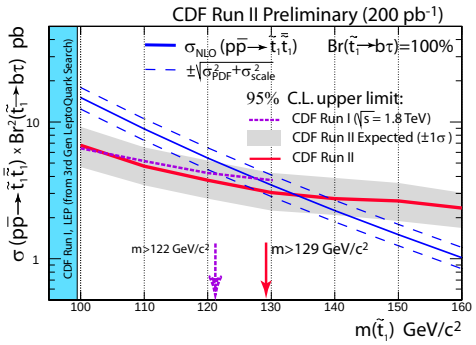

Figure 10. Exclusion limit on production of $p\bar{p} \to \tilde{t}_1\tilde{t}_1$ assuming $Br(\tilde{t}_1 \to b\tau) = 100\%$ in the cross-section versus $M(\tilde{t}_1)$ plane. The band indicates the expected limit, while Run I limit is shown as a dashed line.

5.5. Third Generation Leptoquarks

While the search for SUSY stop pair production excludes scalar leptoquarks decaying to $b\tau$ with mass of $m_{LQ} > 129$ GeV/c^2, leptoquark phenomenology allows a variety of leptoquark species, both scalar and vector ones. An analysis searching for third generation vector leptoquarks with the same experimental signarure of $\tau\tau bb$ is currently underway at CDF. Vector leptoquark production is expected to have a noticeably higher production cross section and harder p_T^{LQ} spectrum compared to the scalar case. If no excess over SM backgrounds were to be found, we anticipate a strong improvement in the excluded mass range for third generation leptoquarks.

5.6. SUSY Chargino-Neutralino Production at High $\tan\beta$

A gold plated signature of SUSY chargino/neutralino pair production and decay is the three lepton final state. There is a strong theoretical and experimental motivation for large $\tan\beta$ in SUSY, e.g. it appears natural that the value of $\tan\beta$, the ratio of VEV's of the Higgs fields that give masses to the up and down-type quarks, should be near the ratio of masses of top and bottom quarks. Larger $\tan\beta$ values result

in dramatic changes in SUSY dynamics leading to tau enriched signatures, e.g. at $\tan\beta \geq 8$ the final leptons in $\tilde{\chi}_1^{\pm}\tilde{\chi}_2^0 \to \nu l \tilde{\chi}_1^0 l l \tilde{\chi}_1^0$ are dominated by τ's, as illustrated in Fig. 11.

While importance of these studies is evident, preliminary CDF projections made in the context of mSUGRA at high $\tan\beta$ have indicated that in order to compete with stringent LEP limits, we need a substantially larger amounts of data than what is available now. One of the main difficulties is the soft spectrum of the tau decay products, which emphasizes the importance of making full use of the detector and trigger capabilities to detect and reconstruct softer τ's.

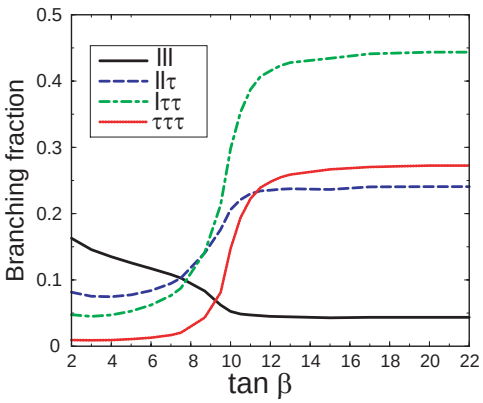

Figure 11. Branching ratio for different modes of trileptons in the final state for $p\bar{p} \to \tilde{\chi}_1^{\pm}\tilde{\chi}_2^0 \to \nu l \tilde{\chi}_1^0 l l \tilde{\chi}_1^0$ production as a function of $\tan\beta$. Note that for $\tan\beta > 8$ tau decay modes become dominant.

6. Conclusions

Physics studies aiming at processes with taus in the final state, while challenging at hadronic colliders, are of great importance in the Tevatron Run II. The CDF experiment has put a significant effort in implementing new triggers and new methods to improve efficiency of hadronic tau selection. In this contribution, a brief description of the methods utilized by CDF for triggering, reconstruction and identification is presented along with preliminary physics results obtained using Run II data. CDF results presented here include electroweak physics as well as the new phenomena searches. With more data being accumulated, we expect improvements in the sensitivity of these measurements as well as a stream of new physics results in the near future.

Acknowledgements

The author would like to thank the organizers for their effort in making this conference a success. Author is also thankful to S. Baroiant, T. Kamon and A. Soha for carefully reading this contribution and their useful suggestions.

REFERENCES

1. The CDF II Detector Technical Design Report, FERMILAB-Pub-96/390-E.
2. S. Kuhlmann et al., Nucl. Instrum. Meth. A518 (2004) 39.
3. T. Affolder et al., Nucl. Instrum. Meth. A526 (2004) 249.
4. S. Baroiant et al., Nucl. Instrum. Meth. A518 (2004) 609.
5. G. Altarelli, B. Mele and M. Ruiz-Altaba, Z.Phys. C45 (1989) 109.
6. R. Mohapatra and G. Senjanovic, Phys. Rev. Lett. 44 (1980) 912.
7. B. Dutta and R. Mohapatra, Physical Review D 59 (1998) 59.
8. D. Acosta et al., The CDF Collaboration, FERMILAB-PUB-04/112-E. Submitted to Phys. Rev. Lett.
9. G. Abbiendi et al., Phys. Lett. B526 (2002) 221
10. M. Muehlleitner and M. Spira, Phys. Rev. D 68 (2003) 117701